HIx system thermodynamic model for hydrogen production by the sulfur-iodine cycle

Mohamed Hadj-Kali, Vincent Gerbaud, Philippe Carles, Jean-Marc Borgard, Olivier Baudouin, Pascal Floquet, Xavier Joulia

HI_X SYSTEM THERMODYNAMIC MODEL FOR HYDROGEN PRODUCTION BY THE SULFUR - IODINE CYCLE

Mohamed Kamel Hadj-Kali[1,2], Vincent Gerbaud[1,2,*], Jean-Marc Borgard[3], Olivier Baudouin[4], Pascal Floquet[1,2], Xavier Joulia[1,2], Philippe Carles[3]

[1]Université de Toulouse, INP, UPS, LGC (Laboratoire de Génie Chimique), 5 rue Paulin Talabot, F-31106 Toulouse Cedex 01 – France

[2]CNRS, LGC (Laboratoire de Génie Chimique), F-31106 Toulouse Cedex 01 – France

[3]CEA, DEN, Physical Chemistry Department, F-91191 Gif-sur-Yvette, France.

[4] ProSim, Stratège Bâtiment A, BP 27210, F-31672 Labège Cedex, France.

* corresponding author

Abstract

The HI_x ternary system (H_2O – HI – I_2) is the latent source of hydrogen for the Sulfur – Iodine thermo-chemical cycle. After analysis of the literature data and models, a homogeneous approach with the Peng-Robinson equation of state used for both the vapor and liquid phase fugacity calculations is proposed for the first time to describe the phase equilibrium of this system. The MHV2 mixing rule is used, with UNIQUAC activity coefficient model combined with of hydrogen iodide solvation by water. This approach is theoretically consistent for HI_x separation processes operating above HI critical temperature. Model estimation is done on selected literature vapor – liquid, liquid – liquid, vapor – liquid – liquid and solid – liquid equilibrium data for the ternary system and the three binaries subsystems. Validation is done on the remaining literature data. Results agree well with the published data, but more experimental effort is needed to improve modeling of the HI_x system.

Keywords: Sulfur – Iodine cycle, HI_x system, phase equilibrium modeling, complex mixing rule

1. Introduction

Hydrogen is undeniably a very attractive energy carrier, superior to others for power generation, transportation and storage. Nowadays, fossil resources account for 95% of hydrogen production. However, given the prospect of an increasing energy demand, of a shortage of fossil resources and of greenhouse gases release limitation, water could be the only viable and long term candidate raw material for hydrogen production. Electrolysis and thermo-chemical cycles are the two leading processes for massive hydrogen production from water. In thermo-chemical cycles, water is decomposed into hydrogen and oxygen via chemical reactions using intermediate elements which are recycled. As the heat can be directly used, these cycles have the potential of a better efficiency than alkaline electrolysis. For massive hydrogen production, the required energy can be provided either by nuclear energy, by solar energy or by hybrid solutions including both.

Among hundreds of possible cycles, the Sulfur – Iodine (S-I) cycle is a promising one [1] in combination with high temperature heat coming from a nuclear reactor. The S-I thermo-chemical cycle is divided into three sections (figure 1): (I) the Bunsen section, where water H_2O reacts with iodine I_2 and sulfur dioxide SO_2 to produce with excess water and iodine, two immiscible liquid aqueous sulfuric-rich and iodhydric acid/iodine-rich phases. The latter is the so-called HI_x phase; (II) the sulphuric acid section where oxygen is produced and (III) the HI_x section where hydrogen iodide concentrates and decomposes to produce hydrogen. Water, iodine and sulfur dioxide are recycled in the system [2].

In 2005, Mathias quoted the ternary system HI – I_2 – H_2O, occurring in Section III among challenges for applied thermodynamics [3]. He wrote: " *…The sulfuric acid decomposition section of …[the S-I]… process can be simulated accurately, but other sections (acid generation and hydrogen iodide decomposition) illustrate the difficulty of modeling phase behavior, particularly liquid-phase immiscibility, in complex electrolyte systems.*"

HI – I_2 – H_2O complexity is well illustrated by literature knowledge:

– Complex phase behavior of the ternary system and the derived binary subsystems:
    - H_2O – I_2 binary is a highly immiscible liquid – liquid system, with solid – liquid equilibrium at low temperatures because of the high melting temperature of iodine (113,6°C) [4],

- H_2O – HI binary is a maximum boiling azeotropic, strong electrolyte system [5] with liquid – liquid equilibrium above approx. x_{HI}=0.34 at 25°C [6],
- HI – I_2 binary exhibits solid – liquid equilibrium [7],
- HI – I_2 – H_2O ternary mixture has two type I liquid – liquid regions [8],

– Many reactions occur, within the liquid solution such as electrolyte decomposition, solvation reactions [9] and poly-iodides formation [10-12] and within the vapor phase with the decomposition of HI in hydrogen and iodine.

– The operating conditions presumed by many authors [13-15] for the unit operations of this section of the cycle are severe (up to 50 bar and above 300°C), making H_2 and possibly HI in supercritical state as seen from table 1.

Where M_W denotes the molecular weight, P_c the critical pressure, T_c, T_b and T_m respectively the critical, the boiling and the melting temperature and ω the acentric factor. Under 1.013 bar and 25°C, HI is vapor, H_2O is liquid, I_2 is solid and H_2 is supercritical. Furthermore, the low critical temperature of hydrogen iodide (150.70°C) and the high melting temperature of iodine (113.60°C) hint that HI could be supercritical under process operating conditions and that iodine could easily crystallize in the process side streams.

The reactive distillation process initially suggested by Roth and Knoche in 1989 [13] is the reference process chosen by CEA [14] for the HI_x section. Until now, no pilot unit has operated under in the expected process conditions (50 bars, 300°C). Such processes are not trivial to design and build, involving choices of suitable holdup and catalyst [16]. So, simulation and modeling remain the sole alternative to evaluate the process performance. The amount of hydrogen produced by hydrogen iodide decomposition ($2HI \leftrightarrow H_2 + I_2$) during the process is closely related to the iodine and hydrogen iodide concentrations in the vapor. Thus the need of an accurate and efficient thermodynamic model of vapor – liquid equilibrium for the HI_x mixture.

The HI_x system thermodynamic model used by Roth and Knoche was proposed by Neumann in 1987 [17] based mostly on total pressure measurements performed at RWTH Aachen [18] and on liquid – liquid equilibrium data tracked through various sources to ref. [8]. These measurements represent a significant achievement, as the HI_x system complexity mentioned above does not facilitate experimental work.

The present paper focuses on the thermodynamic modeling of the HI_x system using VLE, LLE VLLE and SLE experimental data available in the literature with the aim that, in addition to capture the system complex features evoked before, the model can be used in the high pressure (20-50 bar) and high temperature (320-

380°C) conditions of the reactive distillation process. The paper is structured as follows: first, a synthesis of available literature experimental data is presented. Then, an overview of thermodynamic phase equilibrium calculations is given in perspective with the existing literature models and the new modeling approach we propose. The parameter estimation procedure is detailed as well. Finally, results are discussed and compared to literature experimental data.

2. Available experimental data

Available experimental data for the ternary system (HI – I_2 – H_2O) and each binary subsystem (H_2O – HI), (H_2O – I_2) and (HI – I_2) are collected in table 2.

Total pressures of H_2O – HI binary mixtures have been measured by Wüster in vapor – liquid equilibrium conditions [19] and mixing enthalpies by Vanderzee and Gier [20]. Like other water – strong acid mixtures, H_2O – HI mixture exhibits a maximum temperature azeotrope (HI mass fraction equal to 57% (0.1573 molar fraction) at 127°C and atmospheric pressure) [5, 21]. For HI concentrations higher than the azeotrope, the vapor phase is very rich in HI. Furthermore, for high temperatures (> 200°C), HI dissociation in the vapor phase into H_2 and I_2 becomes significant [22, 23]. Wüster [19] quoted that experimental data on the right side of the azeotrope at temperatures above 170°C were discarded because the HI vapor decomposition led to inaccurate measurements. Wüster originally published 119 experimental points (P,T,**x)** and iso-composition correlations giving the saturation pressure dependence versus temperature for different HI mass fractions. Engels published in DECHEMA series [9] a monograph about solvation modeling including the H_2O – HI system but with only 80 points of Wüster's work.

Atmospheric vapor – liquid bubble and dew equilibrium curves of H_2O – HI were measured by Sako and coworkers in 1985 [24] and earlier by Carrière and Ducasse in 1926 [25]. Isothermal vapor – liquid – liquid equilibrium curve at 25°C was published by Haase *et al.* [6]. However, Haase [6] data report the H_2O – HI azeotrope at x_{HI}=0.146 (HI mass fraction of 54.8 %) at 25°C and 0.0166 bar. This is not consistent with other measures. The Pascal monograph [5] reports a x_{HI}=0.1768 (60.4% in mass) around 15–19°C (no pressure reported) and x_{HI}=0.1651 (58.4% in mass) at 100°C. Data of CRC handbook [21] (x_{HI}=0.1573; 57.0% mass at 127.0°C and 1 atm), Sako [24], Carrière and Ducasse [25] (x_{HI}=0.1557; 56.7% mass at 126.5°C and 1 atm), and Wüster [19] agree also that the azeotrope molar and mass fraction increases as pressure is reduced. Therefore, Haase's azeotropic composition is seemingly too low.

However, Haase and coworkers [6] isothermal vapor – liquid equilibrium curves, (P, **x**, **y**) give clear evidence of a H_2O – HI vapor – liquid – liquid equilibrium at 25°C and 7.47bar between x_{HI}=0.346 and x_{HI}=0.995. Unpublished liquid – liquid equilibrium data confirm the H_2O – HI miscibility gap at 24°C/7.3bar and 70°C /17bar in pages 3-55 to 3-63 of reference [8]. Neumann [17] extracted imprecise composition values at five temperatures 70°C, 100°C, 120°C, 136°C and 149°C, likely from a rough sketch of the assumed liquid – liquid equilibrium profiles of the ternary mixture H_2O – HI – I_2 reported in page 3-64 in reference [8].

Pascal [5] reported solid – liquid equilibrium of H_2O – HI mixtures originally published by Pickering [26] (see figure 2). The three eutectic points location tells us that at the azeotropic composition (x_{HI}=0.157, 57.0%mass), solidification leads to hydrated hydrogen iodide crystals (HI, $4H_2O$). Evidently, the hydration number decreases as the H_2O molar fraction decreases because there are not enough water molecules to hydrate HI: the (HI, $4H_2O$) hydrate (x_{HI}=0.20, 64%mass) melts at -36.5°C; the (HI, $3H_2O$) hydrate (x_{HI}=0.25, 70.3%mass) melts at -48.0°C and the (HI, $2H_2O$) hydrate (x_{HI}=0.333, ≅78%mass) melts at -43.0°C. That information will be considered with the hydration of HI in liquid H_2O – HI mixtures discussed later.

For the binary H_2O – I_2, Kracek [4] measured the solubility of solid iodine in water and put in evidence a miscibility gap at 112.3°C up to at least 210°C. At 112.3°C, the light aqueous liquid phase contains x_{I2}=0.0005 and the heavy iodine liquid phase x_{I2}=0.98.

For HI – I_2 O'Keefe and Norman [7] measured the solubility of iodine in HI at five different temperatures (between 25°C and 90°C). These authors highlight that HI – I_2 solutions follow an ideal behavior quite closely, a claim that we reexamine later.

280 equilibrium total pressure measurements of the H_2O – HI – I_2 ternary mixture for a [HI]/[H_20] ratio up to 19.4% and various iodine concentrations are found in the manuscript of Neumann [17]. A synthesis of these results has been published by Engels and Knoche as correlations of the total pressure at equilibrium versus the temperature for several couples of HI and iodine molar fractions [18].

General Atomics report [8] of liquid – liquid equilibrium isopiestic measurements of the ternary mixture H_2O – HI – I_2 confirms a first ternary miscibility gap between water and hydrogen iodide in the presence of iodine through 19 measurements between ≈24°C/7.0bar and 152.1°C/62.2bar from pages 3-55 to 3-63 in ref. [8]. They also hint at a second miscibility gap between water and iodine in the presence of hydrogen iodide above the iodine melting point without providing the relevant ternary data. The second partial miscibility

region reduces as HI concentration increases, probably because of the formation of polyiodides ions like I_3^- [10,11].

All literature data are summarized in table 2 where it is shown which data are used for the model parameter estimation and which are used for its validation.

In addition, several authors have reported the occurrence of endothermic HI decomposition in the vapor phase ($2HI \leftrightarrow H_2 + I_2$), clearly evidenced by a violet coloration characteristic of vapor iodine, both in the binary H_2O – HI [19] and the ternary H_2O – HI – I_2 [18]. High hydrogen iodide molar fraction in the vapor phase occurs for HI liquid molar fraction above the H_2O – HI azeotrope and favors the dissociation. High iodine molar fraction in the vapor phase reduces this dissociation according to the Le Chatelier's principle. Furthermore, HI dissociation reaches equilibrium very slowly [22,23] making difficult to assess the exact quantity of each species.

Palmer and Lietzke [10,11] evaluated poly-iodide formation in the low iodine content in water. Although no precise measurement is available for the ternary H_2O – HI – I_2 mixture, this phenomenon may cause significant dissolution of iodine in H_2O – HI solutions. That would result in a lower iodine molar fraction in the vapor phase, enhancing the suspected HI decomposition in favor of hydrogen production.

3. Model description

3.1. Thermodynamic models background

At constant temperature and pressure, mixture vapor – liquid equilibrium is expressed by equality between liquid and vapor chemical potentials (alternatively fugacities) of each component within the two phases:

$$f_i^V\left(T,P,\bar{\mathbf{y}}\right) = f_i^L\left(T,P,\bar{\mathbf{x}}\right) \quad (1)$$

Where $\bar{\mathbf{x}}$ and $\bar{\mathbf{y}}$ refer to the liquid phase *L* and the vapor phase *V* composition respectively.

Two approaches are commonly used to express the fugacity of each phase [27,28]:

1. In a homogeneous (ϕ–ϕ) approach, the reference state is the perfect gas and is the same for both vapor and liquid phases. Each phase fugacity is calculated by means of components fugacity coefficients ϕ_i from an unique equation of state (EoS):

   $$\phi_i^V\left(T,P,\bar{\mathbf{y}}\right)\cdot y_i = \phi_i^L\left(T,P,\bar{\mathbf{x}}\right)\cdot x_i \quad (2)$$

   Our model is based on this approach.

2. In a heterogeneous ($\gamma-\phi$) approach, vapor and liquid phases are handled differently. For the vapor phase, the reference state is the perfect gas and vapor fugacities f_i^V are obtained from an EoS. For the liquid phase, the reference state is an ideal mixture and liquid fugacities f_i^L are calculated by introducing activity coefficients γ_i, derived from a G^{ex} molar excess Gibbs energy model, to take into account the possible non-ideality of the liquid phase. That gives:

$$\phi_i^V(T,P,\bar{\mathbf{y}})\cdot y_i\cdot P=\gamma_i(T,\bar{\mathbf{x}})\cdot x_i\cdot f_i^{0L}(T,P) \quad (3)$$

Where $f_i^{oL}(T,P)$ expresses the fugacity of component i in one chosen reference state, calculated from the vapor pressure law:

$$f_i^{0L}(T,P)=\phi_i^{0V}(T,P,\bar{\mathbf{y}})\cdot P_i^0(T) \quad (4)$$

Literature models of the HI_x section [17,29,30,31] are based on this approach.

The heterogeneous approach is well suited for strongly non ideal mixtures, but recommendation is to use it far from the critical region. At high pressure, pressure correction like Poynting's factor can be used in $f_i^{0L}(T,P)$. Above the critical point of a component, its vapor pressure law has to be extrapolated. Besides, the heterogeneous approach does not handle correctly mixture critical points above one component's critical point, which in the S-I cycle holds for H_2 and happens for HI at T > 150°C.

On the other hand, the homogeneous approach guarantees the continuity between the two phases at the critical point and requires no extrapolation above and predicts mixture critical points. However, when using simple Lorenz-Berthelot mixing rules, this approach is only appropriate for weakly polar mixtures.

To combine the advantages of both approaches, Huron and Vidal [32] proposed a EoS/G^{ex} homogeneous formalism in which both the liquid and the vapor are modeled by an equation of state but with mixing rules based on the use of activity coefficient models calculation. Unfortunately, published binaries interaction parameters at low pressure with the heterogeneous approach cannot be reused because the HV rule is set on an infinite pressure reference state basis. Then, Michelsen [33,34] proposed the Modified Huron-Vidal (MHV) formalism. He chose a zero pressure reference (ZRP), that could allow to reuse as such all the binary interaction parameters previously published in the literature for the calculation of activity coefficients, or to use a predictive model like UNIFAC [35] and thus make the EoS/G^{ex} model predictive.

There are two MHV1 and MHV2 models as well as other ZRP EoS/G^{ex} models [27,36], which differ mostly in their expression of the function of the reduced attractive-term parameter, α. The MHV2 model complex mixing rule [34] has a quadratic form of α that was estimated within the range $\alpha \in \{8 - 18\}$:

$$q_1\left(\alpha - \sum x_i \alpha_i\right) + q_2\left(\alpha^2 - \sum x_i \alpha_i^2\right) = \frac{G^{ex}(T, P = 0, x_i)}{RT} + \sum x_i Ln \frac{b}{b_i} \qquad (5)$$

With: $\alpha = \frac{a}{bRT}$, $\alpha_i = \frac{a_i}{b_i RT}$ and G^{ex} the excess Gibbs energy model. q_1; q_2 are numerical coefficients of the mixing rule, depending on the equation of state that is used; a, b, a_i and b_i are the attractive and covolume parameter of the equation of state chosen.

However, Kalospiros *et al.* [36] quoted that ZRP EoS/G^{ex} models perform poorly when applied to systems with components that differ appreciably in size, more specifically that differ in α_i values. Indeed, for such mixtures, significant differences arise between the EoS/G^{ex} model and the G^{ex} at zero pressure, that can only be reduced by both a better fit of the real α variation by an α approximate equation and a better fit of the approximate equation differential versus α. They demonstrated that the MHV2 rule could not really be improved for asymmetric mixtures by fitting the quadratic function over a wider α range because a quadratic form cannot match the α derivative, a reason for which it fails dramatically to predict accurate infinite activity coefficients values. The two new fits proposed as solutions are however not conclusive according to their own comments.

We now review the most popular existing HI_x models (Neumann's NRTL modified model and NRTL electrolyte models) before developing the new model.

3.2. HI_x Neumann's model

3.2.1. Engels solvation model basis

Engels solvation model is based on the concept that ions exist in solution only within a stable solvent cloud. The new molecule clusters called "complexes" C are made by the reaction of m solvent molecules S with one electrolyte E molecule according to the expression:

$$mS + E \leftrightarrow \upsilon C \qquad K = \frac{a_C^{\upsilon}}{a_E \times a_S^m} = \frac{\gamma_C^{\upsilon}}{\gamma_E \times \gamma_S^m} \times \frac{x_C^{\upsilon}}{x_E \times x_S^m} \qquad (6)$$

Where υ is the number of dissociation products of one electrolyte molecule; x_i is the molar fraction of the species i and a_i, γ_i their activity and activity coefficient respectively.

Such a model rely upon a symmetric convention for the electrolyte and for the solvent, applicable over the entire composition range. Under dilute electrolyte conditions, the excess of solvent favors the complete dissociation and solvation of the electrolyte. Near pure electrolyte, lack of solvent leaves the electrolyte undissociated. This is consistent with the discussion on the solid – liquid equilibrium of the binary H_2O – HI, given in figure 2 [26].

The Engels solvation concept significantly simplifies the model development, since no charged species are considered in the liquid phase and the activity coefficient model adopted is only based upon the short range interactions between molecules. The parameters are principally the molecule-molecule interaction terms, including Engels' complex molecule, both with the solvation number m.

For the binary mixture H_2O – HI, Engels took the solvation number m equal to 5 and wrote the solvation reaction under the form :

$$5\ H_2O\ +\ HI \quad \leftrightarrow \quad 2\ C \qquad\qquad K = \frac{a_C^2}{a_{HI} \times a_{H2O}^5} \qquad (7)$$

Engels's model dimensional analysis is similar to the strict thermodynamic description of an electrolyte dissociation followed by solvation of the cation. For example, for H_2O – HI, we write:

$$HI \quad \leftrightarrow \quad H^+ + I^- \qquad K_{dissociation} = \frac{a_{H^+} \cdot a_{I^-}}{a_{HI}} \qquad (8)$$

$$mH_2O + H^+ \quad \leftrightarrow \quad (m\text{-}1)H_2O),\ H_3O^+ \qquad K_{solvationH^+} = \frac{a_{\left((m-1)H_2O, H_3O^+\right)}}{a_{H^+} \cdot a_{H_2O}^m} \qquad (9)$$

$$mH_2O + HI \quad \leftrightarrow \quad [(m\text{-}1)H_2O),\ H_3O^+;\ I^-] \qquad K = \frac{a_{I^-} \cdot a_{\left((m-1)H_2O, H_3O^+\right)}}{a_{HI} \cdot a_{H_2O}^m} \qquad (10)$$

The equilibrium constants of equations 7 and 10 are equivalent with m = 5 and a complex 2C that would be like $[(m\text{-}1)H_2O),\ H_3O^+;\ I^-]$.

The hydronium ion H_3O^+ exists in aqueous solutions, with a hydration number that may vary upon conditions [37]. Furthermore, molecular dynamic simulations have shown that cation hydrates in solution are dynamic clusters where H_2O molecule on the cluster surrounding can be replaced by bulk solvent molecules [38].

This model was first used successfully by Engels with the Wilson activity coefficient model [9] to describe the vapor – liquid phase equilibrium of the binary mixture H_2O – HI.

3.2.2. Neumann's NRTL modified model description

In conjunction with the solvation reaction, Wilson's model proposed by Engels is intrinsically unable to describe liquid phase demixtion [28] that occurs in the HI_x system, though. To study the ternary mixture H_2O – HI – I_2, Neumann [17] used a heterogeneous approach with a perfect gas vapor phase and, for the non ideal liquid phase, Engels' solvation combined with a modified NRTL model that is suitable to model liquid – liquid phase equilibrium. Above HI critical temperature, its vapor pressure law is extrapolated.

The original NRTL model activity coefficient expression of component i [39] is:

$$\frac{g^{Ex}}{RT} = ln\,\gamma_i = \frac{\sum_{j=1}^{N}\tau_{ji}G_{ji}x_j}{\sum_{j=1}^{N}G_{ji}x_j} + \sum_{j=1}^{N}\frac{G_{ij}x_j}{\sum_{k=1}^{N}G_{kj}x_k}\left[\tau_{ij} - \frac{\sum_{k=1}^{N}\tau_{kj}G_{kj}x_k}{\sum_{k=1}^{N}G_{kj}x_k}\right] \qquad (11)$$

Where $G_{ji} = exp(-\alpha_{ji}\tau_{ji})$

Components i and j binary interaction is defined by three parameters: τ_{ij}, τ_{ji} and the non-randomness parameter α_{ij}, with α_{ij} set equal to α_{ji}. Neumann modified the NRTL model [17], considering $\alpha_{ji} = -\alpha_{ij}$, and a specific temperature dependence for τ_{ij} and τ_{ji}. Furthermore he identified one set of binary interaction parameters to be used for temperatures below 150°C and one set above 150°C. Notice that the 150°C is close to the HI critical temperature (150.70°C)). He also identified a solvation equilibrium constant $K_a(T)$ (equation 8) applicable to any temperature.

Neumann's model was recently revisited by Yoon *et al.*, [40] who introduced a new NRTL model modification with independent and positive α_{ji} and α_{ij} and evaluated the HI dissociation impact on the calculations. They estimated on Neumann's monograph data [17], three different sets of NRTL binary interaction parameters and of solvation constant values, respectively for the binary H_2O – HI and for the ternary H_2O – HI – I_2 below and above 150°C.

Neumann's model was formerly used by several authors [14,15] to simulate a reactive distillation process for the recovery of hydrogen, designed with a column composition profile located on the H_2O – HI – I_2 mixture temperature crest where the mixture has a single liquid phase in equilibrium with the vapor phase. The phase diagrams can be calculated with confidence on the left-hand side of the binary H_2O – HI azeotrope

and when the iodine content is low. Uncertainties remain for high iodine contents and high temperatures [15]. The nominal pressure proposed in these works was 22 bars, following Roth and Knoche suggestion that this would favor hydrogen production [13]. This pressure is below any of the three components critical pressure, but the mixture equilibrium temperature is above the HI critical temperature (150.70°C).

3.2.3. HI_x Neumann's model limitations

3.2.3.1. Vapor pressure law extrapolation:

In the heterogeneous approach vapor – liquid equilibrium equation (3) $f_i^{0L}(T,P)$, the fugacity of the pure liquid of each constituent at the temperature and pressure of the system, is expressed in terms of the vapor pressure laws $P_i°(T)$ usually estimated on vapor – liquid equilibrium data of pure components. However, for HI_x mixtures temperature above HI supercritical temperature ($T_{c,HI}$=150.70°C), HI vapor pressure law must be extrapolated in order to compute any equilibrium above this temperature for a mixture containing HI. The literature propose several laws consistent together:

o Engels proposed:

$$P_{HI}°(bar) = 1.01325 \cdot 10^{\left(\frac{T-T_b}{T}\right)\left[4.43-0.48\cdot\left(\frac{T-T_b}{T_b}\right)+0.5\cdot\left(\frac{T-T_b}{T_b}\right)^2\right]} \quad (T \text{ and } T_b \text{ in K}) \qquad (12)$$

T_b denotes the boiling temperature of HI equal to -35.55°C.

o Neumann added an extrapolated expression above HI critical temperature:

$$P°(bar) = 10^{\left(4.3764-\frac{1040.31}{T}\right)} \qquad (13)$$

o DIPPR saturation pressure law for HI was used in other works [15] and is given by [40]:

$$P°(Pa) = exp\left(54.233 - \frac{3342.1}{T} - 5.5756 \times ln(T) + 0.0078 \times T\right) \quad (\text{with } T \text{ in K}) \qquad (14)$$

The vapor – liquid equilibrium homogeneous approach doesn't use nor requires any extrapolation of the vapor pressure law.

3.2.3.2. vapor – liquid equilibrium calculation above HI critical point

With or without any vapor pressure extrapolation, a heterogeneous approach model is intrinsically unable to compute correctly any mixture critical line. Phase equilibrium for any mixture containing HI, above HI critical

temperature cannot reach 100% HI because under such conditions, pure HI is supercritical and not involved in any phase equilibrium. A homogeneous approach can predict so but a heterogeneous one cannot from theory [28]. Within a reactive distillation column operating above HI critical temperature, the heterogeneous approach could over predict the HI content in the vapour phase, with consequences on the estimated hydrogen content obtained from the dissociation of HI.

3.2.3.3. Perfect gas hypothesis

Assuming a perfect gas vapor phase, as did Neumann or Engels, is dubious regarding the high total pressures achieved. Preliminary calculation of the compressibility factor for the ternary system H_2O – HI – I_2 by a cubic equation of state like SRK or PR at pressures higher than 10 bars hints at values close to 0.90 rather than perfect gas unity value.

3.3. HI_x NRTL electrolytic models

By using a solvation model with no explicit ionic species together with an activity coefficient model for the non ideal liquid phase, Engels and Neumann's HI_x models rely upon a symmetric convention for all components in the liquid phase, namely that the activity coefficient γ_i goes to 1 as the component fraction x_i goes to 1. That convention enables to explore the whole composition range without limitations.

But strong acidic mixture like the HI_x one are often described with explicit ions. The electrolyte-NRTL model developed by Chen [42,43] does it and combines the Pitzer-Debye-Hückel model [44] for long-range ion-ion electrostatic interactions with the NRTL theory [39] for short-range energetic interactions among the species in electrolyte solutions. Such an electrolyte model uses an asymmetric convention distinguishing solute and solvent:

$$\begin{aligned} &\gamma_{solvent} \to 1 \quad as \quad x_{solvent} \to 1 \\ &\gamma_{solute} \to 1 \quad as \quad x_{solute} \to 0 \end{aligned} \tag{15}$$

As the NRTL equation was developed using a symmetric convention, it is associated to the electrolyte Pitzer-Debye-Hückel model by asymetrizing it using the usual formula:

$$\gamma_i^{sym} = \gamma_i^{asym} \cdot \gamma_i^{\infty} \tag{16}$$

Where γ_i^{∞} is the infinite dilution activity coefficient.

3.3.1. Brown's electrolyte model (2001)

Brown and co-workers [29,30] used Chen's electrolyte-NRTL model to describe the liquid phase by considering the presence of H_3O^+, OH^- and I^- ions in the mixture:

$$H_2O \leftrightarrow H_3O^+ + OH^- \quad (17)$$

$$HI + H_2O \leftrightarrow H_3O^+ + I^- \quad (18)$$

Electrolyte parameters and NRTL binary interaction parameters were estimated from experimental data of Kracek [4], Wüster [19], Engels [18] and O'Keefe and Norman [7]. Good representation of all binary subsystems is achieved, including liquid – liquid demixtion and a maximum deviation error for the total pressure of the ternary system about 30% is obtained. The perfect gas model is used for the vapor phase.

3.3.2. Annesini's electroyte model (2007)

Annesini *et al.* [32] combined the Redlich-Kwong equation of state for the vapor phase and Chen's electrolyte-NRTL activity coefficient model for the liquid phase. In order to describe the vapor – liquid equilibrium in a wide range of composition, HI has been chosen as the Raoult reference state.

3.3.3. NRTL electrolytic models limitation

Former limitations of heterogeneous vapor – liquid equilibrium approach still hold for NRTL electrolytic models, namely the extrapolation of vapor pressure law and an incorrect behavior of mixture critical lines. The asymmetric convention brings an additional limitation to use the model over the entire composition range. Chen's electrolyte-NRTL model claims accurate prediction of activity coefficient up to 16 mol/kg of solvent for strong acid electrolytes like HCl or H_2SO_4 [45], which is still far from pure electrolyte. It remains still questionable to choose an infinite dilution convention for the solute activity coefficient ($\gamma_{solute} \rightarrow 1$ when $x_{solute} \rightarrow 0$) when one expects to predict fluids behavior with almost pure electrolyte.

3.4. New homogeneous approach EoS/G^{ex} model

Based on the literature survey, a homogeneous approach with the MHV2 complex mixing rule incorporating UNIQUAC model [46,47] and Engels solvation is proposed to model the HI_x system.

First, two cubic EoS are tested, Soave-Redlich-Kwong (SRK) and Peng-Robinson (PR) equation of state, with Boston-Mathias modification of the $\alpha(T)$ function [48], reputed to perform better at high pressure than

the original cubic EoS α(T) function. PR predicts experimental vapor pressures of pure components with the least deviation as shown in the table 3 below and is finally selected.

The MHV2 complex mixing rule [34] (equation 5) is chosen with no modification of the alpha estimated function. The new excess Gibbs energy model (G^{ex}), called UQSolv, is a combination of the UNIQUAC activity coefficient model (equation 19) with Engels' model solvation (equation 6) of HI by H_2O.

$$\frac{g^{Ex}}{RT} = f_{combinatorial}(\bar{x}, r, q) + f_{residual}(\bar{x}, q', A_{ij}, A_{ji}) \quad (19)$$

The UNIQUAC model sums two contributions (equation 19). The combinatorial term handles molecule size difference effects whereas the residual term accounts for fluid interactions [46]. Steric effects are expected as iodine and water molecular weights and sizes are quite different (254 $g.mol^{-1}$ vs 18 $g.mol^{-1}$ respectively). Defined as the Van der Waals volume and the area of the molecule, UNIQUAC structural parameters *r* and *q* (*q'*=*q*) are taken from the literature [49] (see table 4). Following UNIQUAC's authors suggestion [46], the solvation complex parameters are calculated from an arithmetic mixing rule of the contribution of each molecule involved in the complex [49].

The ZRP EoS/G^{Ex} model presumes that estimated binary interaction parameters A_{ij} and A_{ji} arising in UNIQUAC's residual term can be used either with a heterogeneous approach (involving standard mixing rule) at low pressure or a homogeneous one (complex mixing rule) at any pressure.

Engels' solvation model is suitable for multiple solvations [9] but we only consider the solvation of HI by H_2O. Polyiodide formation in the HI_x system is strongly suspected when water is present [10,11] but is discarded because experimental data on polyiodide in HI_x mixtures is missing to allow calibration of the relevant solvation constant. Brown and Annesini's electrolyte model have also set it aside.

4. Parameter estimation procedure

The parameter estimation procedure deals separately with each binary subsystem before refining the parameters of the ternary system. Furthermore, the estimation is done using a heterogeneous approach, namely the UQsolv model for the liquid phase and the PR-Boston Mathias for the vapor phase. The use of the UQSolv model within the MHV2 complex mixing rule and with the PR-Boston Mathias homogeneous approach is recommanded and used for the H_2O – HI – I_2 ternary system and for the binary system H_2O – HI, especially for temperatures higher than the critical HI temperature and high pressure. High pressure

calculations are not reported here because experimental data is not available to validate predictions. The UQsolv model alone is used for SLE, and LLE calculations.

For all binary mixtures, H_2O – I_2 and HI – I_2 and H_2O – HI UNIQUAC binary interaction parameters are estimated. For H_2O – HI, the hydrogen iodide solvation by water parameters are estimated in parallel as well. Finally, ternary H_2O – HI – I_2 experimental data are used to refine the estimated parameters. Table 2 recall the data used for the estimation procedure and for the model validation.

The model development is achieved within Simulis® Thermodynamics environment, a thermo physical properties calculation server provided by ProSim [50] and available as an MS-Excel add-in. As Simulis® is a CAPE-OPEN compliant object, the model could be used in any process simulator matching the CAPE-OPEN thermodynamic standard 1.0 or 1.1.

Binary interaction parameters are estimated from N_p experimental data points by minimizing the quadratic relative criterion between calculated and experimental thermodynamic properties Y:

$$Criterion = \frac{1}{N_p}\sum_{N_p}\left(\frac{Y_{exp} - Y_{cal}}{Y_{exp}}\right)^2 \qquad (20)$$

Comparison of the model with experimental data is presented below and is done with the final set of parameter values. Those are not provided due to confidentiality clause.

5. Results and discussion

5.1. H_2O – I_2 mixture

For water – iodine, interaction parameters are estimated using experimental liquid – liquid equilibrium data of Kracek [4]. Figure 3 displays the experimental equilibrium temperature versus iodine molar fraction in each liquid phase, comparing our UQSolv model and the Neumann's modified NRTL model. The SLE is predicted using the fusion enthalpy correlation and melting temperature data available in the DIPPR data bank [41].

The iodine rich phase is well estimated by both the UQSolv and Neumann's models. The aqueous liquid phase composition is better modeled by the new UQSolv model than by Neumann's model. Furthermore, UQsolv achieves without any further adjustment a remarkable prediction of the experimental solid iodine solubility in water.

Better aqueous liquid phase description than what is displayed in figure 3 was obtained but that degraded the iodine liquid phase description and the corresponding parameter set was not retained.

5.2. HI – I_2 mixture

Hydrogen iodide – iodine interaction parameters are estimated using the experimental solid – liquid – equilibrium data of O'Keefe and Norman [7] up to the iodine melting temperature. Figure 4 displays the mass composition of iodine versus temperature at equilibrium. The UQSolv model fits nicely the experimental data, as the NRTL electrolytic model did [29]. The ideal liquid model (unity activity coefficient in equation 3) and the "standard UNIQUAC" models (null binary interaction parameters) are also displayed for comparison on the figure. That shows how the size effects account for a significant deviation from the ideal case and how non ideal is this mixture.

5.3. H_2O – HI mixture

Water - hydrogen iodide UQSolv parameters are estimated using the experimental vapor – liquid equilibrium data of Wüster [19] reported by Engels in the DECHEMA monograph [9].

5.3.1. solvation parameters estimation

At first, solvation parameters are estimated only on the basis of experimental data on the left side of the azeotrope (x_{HI} < 0.15) which are more accurately known than the right side. Engels' solvation equation (6) requires a solvation number (*m*) and A and B parameters for the solvation equilibrium constant K_{solv}:

$$K_{solv} = exp\left(A + \frac{B}{T}\right) \quad (T \text{ in K}) \tag{21}$$

Both Engels and Neumann set the solvation number equal to 5. Estimation of m=3.8 was done together with the binary interaction parameters. We obtained a value of 3.8, consistent with the $HI,4H_2O$ solid hydrate found at the azeotrope composition reported in figure 2 [26] and discussed in a previous section. Figure 2 hints that H_2O – HI liquid solution has some tangible but variable degrees of solvation. Engels' solvation equation requires a single value though.

Comparison between Engels', Neumann's and our solvation curves shows that our solvation constant approaches Engels' one at high temperatures and Neumann's one at low ones (see figure 5). We have noted in preliminary calculations (not shown) that using the solvation constant alone, without any binary

interaction parameters, allows to estimate correctly the H_2O – HI azeotropic point. Vidal [28] indicated that maximum temperature azeotrope in binary mixtures like water – strong acids are due either to solvation phenomenon or hydrogen bond formation in the solution. However, it is a combination of solvation with binary interaction that fits the best the data.

5.3.2. Binary interaction parameters estimation

H_2O - HI binary interaction parameters are estimated on Wüster's experimental data on the left side of the azeotrope (x_{HI}<0.15). Data on the right side of azeotrope are assigned a high experimental uncertainty based on Wüster's comments and on the author's own experience (see figure 6). Indeed, if measurements are done in a constant volume cell, as is usual, introduction of a mixture of defined composition *z* in the cell implies vaporization once the experiment temperature is achieved. Thus the exact liquid and vapor composition in equilibrium can only be known through an evaluation of the vaporization. That could be done by a flash calculation but it would requires a thermodynamic model, that we are precisely looking for. That effect is even more pronounced on the right side of the maximum boiling azeotrope where the vapor is very rich in the least volatile compound HI as vapor – liquid equilibrium data indicate. Furthermore, HI decomposition in the vapor phase likely occurs and as a kinetically driven reaction, is difficult to consider during the calculation unless hydrogen production experimental information is known.

Figure 6 displays the reasonable fitting of the HI mass fraction data of Wüster with the PR/MHV2/UQSolv model. On the right handside of the azeotrope, the vapor pressure is overestimated though but from the discussion above, we may expect that if Wüster's reported composition is the overall composition fed to the measurement cell, the precise bubble composition would then be on the left of the reported point.

Figure 7 compares the predicted bubble and dew curves with experimental HI molar fraction data at atmospheric pressure [25]. As expected from our estimation procedure, prediction of the bubble pressure agrees well up to the azeotropic point but deviates significantly on the right of the azeotrope where the experimental data are still uncertain. Neumann's model does not predict the H_2O – HI immiscibility at 1 atm. Neumann sketched in his report the isothermal vapor – liquid – liquid equilibrium at 70°C with an immiscibility region at approx. 20-21 bar [17].

Vapor – liquid – liquid and liquid – liquid equilibrium predictions of the new model are also displayed in figure 7, using UQSolv model or PR/MHV2/UQSolv model. Differences occur, especially in the calculation of the

liquid – liquid equilibrium span near the vapor – liquid – liquid temperature -35°C and are discussed below in the paragraph about liquid – liquid equilibrium calculation.

Figure 8 compares the predicted and experimental [6] bubble pressure at 25°C. In this figure, a noteworthy deviation is observed at the right side of azeotrope probably accentuated by the inaccurate azeotrope measurement in this work, as mentioned earlier.

The prediction of the maximum boiling temperature azeotrope composition is in agreement with the literature reported in the Pascal monograph [5] (table 5).

Table 5. Calculated and experimental H_2O – HI azeotrope at different temperatures.

Experimental [Pascal, 1960]			UQsolv model		
HI molar Fraction	T_{azeo} (°C)	P_{azeo} (atm)	HI Molar Fraction	T_{azeo} (°C)	P_{azeo} (atm)
15.73*	127*	1	15.68	128.24	1
16.51	100	-	16.20	100.00	0.360
17.68	15-19	-	17.79	15.00	0.004

A significant achievement of the new model is the quantitative prediction at 25°C of the vapor – liquid – liquid equilibrium ($x_{HI}^{(1)}$ = 0.360 $x_{HI}^{(2)}$ = 0.992 at 7.77atm with PR/MHV2/UQsolv and $x_{HI}^{(1)}$ = 0.330 $x_{HI}^{(2)}$ = 0.992 at 7.74atm with UQSolv alone) measured experimentally by Haase *et al.* at 25°C ($x_{HI}^{(1)}$ = 0.346 $x_{HI}^{(2)}$ = 0.9995 at 7.56atm) [6]. Notice in that case the PR/MHV2/UQSolv discrepancy versus UQSolv is less pronounced than for VLLE and LLE below -35°C at 1 atm but this near agreement at 7.77 atm is merely fortuitous.

We recall that a ZRP EoS/G^{ex} model should theoretically reduced to G^{ex} model at zero pressure. The reason for which it doesn't when computing VLLE or LLE was discussed in the thermodynamic model background section. It is attributed to the use ZRP EoS/G^{ex} for mixtures containing compounds of significant different sizes, like large I_2, HI and small H_2O molecules.

Now, either the PR/MHV2/UQSolv or the UQSolv model agrees reasonably with the H_2O - HI liquid – liquid equilibrium data of General Atomics [8] (x_{HI}^{1}=0.359 at 24°C and x_{HI}^{1}=0.308 at 70°C with PR/MHV2/UQSolv and x_{HI}^{1}=0.330 at 24°C and x_{HI}^{1}=0.331 at 70°C with UQSolv vs. experimental x_{HI}^{1}=0.33 at 24°C and $x_{HI}^{(1)}$ = 0.30 at 70°C). The extrapolated data of Neumann at 100°C, 120°C, 136°C and 149°C are not used here and were falsely assumed as being experimental data in ref. [40] where they were used for validation. The validation has shown so far the adequacy of the PR/MHV2/UQSolv to represent VLE data but more experimental LLE data would be needed to validate the use of either PR/MHV2/UQSolv or UQSolv model for computing phase equilibrium with liquid – liquid split. We recall that the reactive distillation process proposed

by Roth and Knoche [13] showed column profile compositions in the vapor – liquid equilibrium region, with no need for VLLE calculations.

5.4. H_2O – HI – I_2 mixture

5.4.1. Parameter estimation

For the ternary system H_2O – HI – I_2, the binary interaction parameters estimated for each binary system and the solvation parameters of hydrogen iodide by water are kept constant. The interaction between iodine and the solvation complex are then estimated using the ternary vapor – liquid equilibrium data.

The final parameter values are not shown due to the confidentiality clause of the funding partner.

5.4.2. Vapor – liquid equilibrium data comparison

The ternary vapor – liquid equilibrium data published by Neumann [17] are well described: the average relative error, the maximum error and the criterion values are respectively 8.2%; 44% and 3.7 for the PR/MHV2/UQSolv model. Those numbers are better than the values obtained with the parameter set proposed by Neumann below 150°C but worse than the one above 150°C. We thus infer that the extrapolated law for the vapour pressure used with the “above 150°C” parameter set of Neumann is reasonable, although it has no theoretical support at all, on the basis of the existing experimental data.

In addition, as the full line shows on figure 9 for the PR/MHV2/UQSolv, we notice a trend to overestimate the data at high pressures. However, one should keep in mind that the same set of parameters is used to describe not only the ternary system but also all binary subsystems as described throughout this paper and their respective SLE, LLE and VLE equilibrium.

5.4.3. Liquid – liquid equilibrium data comparison

Figure 10 compares the new model predictions at 121.5°C and 43 bar with the experimental data at 120.9; 121,5 and 121.7°C under approx. 43 bar in ref. [8].

The MHV2/UQSolv model underpredicts the HI composition and overpredicts the H_2O composition in the HI-lean phase for two of the three tie lines but the slope of the tie line is reasonably predicted. The model also predicts at 43bar the second partial miscibility region between H_2O – I_2 in presence of HI, which is postulated

in reference [8]. Neumann's model could not predict such data but NRTL electrolytic model of Brown *et al.* [29,30] did.

6. Conclusions

The so-called HI_x (H_2O – HI – I_2) system has been modeled by using a ZRP EoS/G^{ex} homogeneous approach. The Peng-Robinson equation of state with Boston Mathias α function holds for both the vapor and liquid phase. To capture the strong non ideal behavior of the mixture, the MHV2 complex mixing rule is used, embedding the UNIQUAC Gibbs excess energy model together with a Engels' solvation equilibrium of HI by H_2O. Literature data are criticized and selected ones are used to estimate the UNIQUAC binary interaction parameters and the solvation constant parameter values. Other are used for validation of the model.

Former models proposed by Neumann, Yoon, Mathias or Annesini based on a heterogeneous liquid/Gibbs excess energy model – vapor/equation of state approach are reviewed. Unlike the new homogeneous approach, they are intrinsically unable to capture the supercritical behavior of HI likely occurring above HI critical temperature of 150.7°C.

Based on the theoretical arguments discussed, the use of a ZRP EoS/G^{ex} homogeneous approach is recommended in place of a heterogeneous G^{ex} model for any VLE calculation above HI critical temperature, 150.7°C. LLE and VLLE calculations could be done with either one approach as ZRP EoS/G^{ex} calculation usually match with G^{ex} calculations at the low pressures under which liquid – liquid phase split may occur. For the HI_x system, this is not true due to large atomic size differences between the HI_x system compounds. The few liquid – liquid equilibrium data do not allow to discriminate between the PR/MHV2/UQsolv and the UQsolv alone models for LLE and VLLE calculations.

The new model successfully represents most of the vapor – liquid, liquid – liquid, solid – liquid, vapor – liquid – liquid experimental data available from the literature, with a unique set of temperature dependent binary interation and solvation parameters, unlike the recent work of Yoon *et al.* who proposed three sets [40]. The largest discrepancy is found for high HI concentration mixtures where experimental data are sparse and uncertain due to the likely dissociation of HI into H_2 and I_2.

In fact, more and accurate detailed composition data are needed to consider system features like the dissociation of HI in the vapor phase but also the probable poly-iodide formation in the liquid phase that could be described by a solvation of HI by I_2. The CEA has recently launched a program to measure the

relevant partial pressures [51], which are necessary to effectively estimate the hydrogen production potential under the reactive distillation process expected conditions (up to 300°C and 50 bars).

7. Acknowledgment

The authors thank Pr. J.P. O'Connell for invaluable discussions on experimental data and theoretical models on the HIx system.

8. References

[1] Funk J.E., Thermochemical hydrogen production: past and present, Int. J. Hydrogen Energy, 2001;26(3):185-190.

[2] O'Keefe D., Allen C., Besenbruch G., Brown L., Norman J., Sharp R. and McCorkle K., Preliminary results from bench-scale testing of a sulfur-iodine thermochemical water-splitting cycle, Int. J. Hydrogen Energy, 1982;7(5):381-392.

[3] Mathias P.M., Applied thermodynamics in chemical technology: current practice and future challenges, Fluid Phase Equilibria, 2005;228-229:49-57.

[4] Kracek F.C., Solubilities in the system water-iodine to 200°C, J. Phys. Chem., 1931;35 :417.

[5] Pascal P., Nouveau traité de chimie minérale. tome 16. chlore, brome, iode, astate, manganese, technetium, rhenium (1960) Edition Masson. 1195 pages

[6] Haase R., Naas H., Thumm H., Experimental investigation on the thermodynamic behavior of concentrated halogen hydrogen acids, Z. Phys. Chem. NF, 1963;37:210-229.

[7] O'Keefe D.R., Norman J.H., The vapour pressure , iodine solubility, and hydrogen solubility of hydrogen iodide – iodine solutions, J. Chem. Eng. Data, 1982;27:77-80.

[8] O'Keefe D.R., Norman J.H., Brown L. and Besenbruch G. GA technologies thermochemical water – splitting process improvements. Final Report 1984, (1984) Report GA A17752.

[9] Engels H., Phase equilibria and phase diagrams of electrolytes, Chemistry data Series, Volume XI, Part I. (1990) Published by DECHEMA. ISBN 3-926959-17-7, 160 pages.

[10] Palmer A.D., Lietzke M.H., The equilibria and kinetics of iodine hydrolysis, Radiochimica Acta, 1982;31:37-44.

[11] Palmer A.D., Ramette R.W., Mesmer R.E., Triiodide ion formation equilibrium and activity coefficients in aqueous solution, Journal of Solution Chemistry, 1984;13(9):673-683.

[12] Calabrese V.T., Khan A., Polyiodine and polyiodide species in an aqueous solution of iodine + KI: Theoretical and experimental studies, J. Phys. Chem. A, 2000;104:1287-1292.

[13] Roth M. and Knoche K.F., Thermo-chemical water-splitting through direct HI decomposition from HI/I2/H2O solutions, Int. J. Hydrogen Energy, 1989;14(8):545-549.

[14] Goldstein S., Borgard J.M., Vitart X., Upper bound and best estimate of the efficiency of the iodine sulfur cycle, Int. J. Hydrogen Energy, 2005;30:619.

[15] Belaissaoui B., Thery R., Meyer X.M., Meyer M., Gerbaud V., Joulia X., Vapour reactive distillation process for hydrogen production by HI decomposition from HI–I2–H2O solutions, Chem. Eng. Proc., 2008;47(3):396-407.

[16] Sundmacher K., Kienle A., 2003, *Reactive distillation status and future directions,* WILEY-VCH, 308 pages ISBN: 978-3-527-30579-7.

[17] Neumann D., Phasengleichgewichte von HJ/H2O/J2 – Lösungen. Lehrstuhl für Thermodynamik, RWTH Aachen, 5100 Aachen (Germany). Master's thesis; January 1987,.

[18] Engels H., Knoche K., Vapor pressures of the systems HI/I2/H2O and H2, Int. J. Hydrogen Energy, 1986;11(11):703-707.

[19] Wüster G., p,v,T – und Dampfdrückmessengen zur Bestimmung Thermodynamischer Eigenschaften Starker Elektrolyte bei Erhöhten Druck, june 1979, Thesis (1979) RWTH Aachen. (in German).

[20] Vanderzee C.E., Gier L.J., The enthalpy of solution of gazeous hydrogen iodide in water, and the relative apparent molar enthalpies of hydriodic acid, J. Chem. Thermodynamics, 1974;6:441-452.

[21] CRC Handbook of chemistry and physics (1988) 69th Edition by CRC Press.

[22] Shindo Y., Ito N., Haraya K., Hakuta T., Yoshitome H., Kinetics of the catalytic decomposition of hydrogen iodide in the thermochemical hydrogen production, Int. J. Hydrogen Energy, 1984;9(8):695-700.

[23] Berndahauser C., Knoche K.F., Experimental investigations of thermal HI decomposition from H2O---HI---I2 solutions. Int. J. Hydrogen Energy, 1994;19(3):239-244.

[24] Sako T., Hakuta T., Yoshitome H., Vapor liquid equilibria for hydrogen iodide – water, nitric acid – water, hydrogen iodide – water – salt and nitric acid – water – salt systems. Kagaku Gijutsu Kenkyusho Hokoku, 1985;80(5):199-203.

[25] Carrière E., Ducasse, Détermination des courbes de bulle et de rosée des mélanges d'acide iodhydrique et d'eau sous une pression de 746 mm de mercure. CR de chimie, 1926;1281-1282.

[26] Pickering S.E., Die Hydrate der Jodwasserstoffsäure 1893;2307-2310.

[27] Sandler S.I., *Models for thermodynamic and Phase Equilibria Calculations* (1994) Marcel Dekker Inc., New York, ISBN 0-8247-9130-4.

[28] Vidal J., *Applied thermodynamic for chemical engineering and oil industry*, (2003) Technip Editions.

[29] Brown L.C., Mathias P.M., Chen C.C., Ramrus D. Thermodynamic Model for the HI-I_2-H_2O System, AIChE Annual Meeting, 4-9 November, 2001.

[30] Mathias P.M., Brown L.C. Thermodynamics of the sulphur-iodine cycle for thermochemical hydrogen production', Presented at 68th Annual Meeting of the Society of Chemical Engineers, Japan, 2003.

[31] Annesini M.C., Gironi F., Lanchi M., Marrelli L., Maschietti M., S-I thermochemical cycle for H2 production: a thermodynamic analysis of the phase equilibria of the system HI-I2-H2O, Proceedings of ICheaP-8, The eigth Italian Conference on Chemical and Process Engineering, 2007.

[32] Huron M.J., Vidal J., New mixing rules in simple equations of state for representing vapour-liquid equilibria of strongly non-ideal mixtures, Fluid Phase Equilibria, 1979;3:255-271.

[33] Michelsen M.L., A method for incorporating excess Gibbs energy models in equations of state, Fluid Phase Equilibria, 1990;60:47-58.

[34] Michelsen M.L., A modified Huron-Vidal mixing rule for cubic equations of state, Fluid Phase Equilibria, 1990;60:213-219.

[35] Fredenslund A., Jones R.L., Prausnitz J.M., Group-contribution estimation of activity coefficients in nonideal liquid mixtures, AIChE Journal, 1975;21(5):1086-1099.

[36] Kalospiros N.S., Tzouvaras N., Coutsikos P., Tassios D.P., Analysis of zero-reference-pressure EoS/GE models, AIChE Journal, 1995;41(4):928-937.

[37] Zavitsas A.A., Properties of Water Solutions of Electrolytes and Nonelectrolytes, J. Phys. Chem. B, 2001;105:7805-7815.

[38] Iyengar S.S. , Petersen M.K., Burnham C.J., Day T.J.F., Voth G.A., The properties of ion-water clusters. I. The protonated 21-water cluster, J. Chem. Phys., 2005;123:084309.

[39] Renon H., Prausnitz J.M., Local compositions in thermodynamic excess functions for liquid mixtures, AIChE Journal, 1968;14(3):135-144.

[40] Yoon H.J., Kim S.J., No H.C., Lee B.J., Kim E.S., A thermo-physical model for hydrogen–iodide vapor–liquid equilibrium and decomposition behavior in the iodine–sulfur thermo-chemical water splitting cycle, Int. J. Hydrogen Energy, 2008;33(20):5469-5476.

[41] Danner R.P., Daubert T.E., DIPPR Project 801, Design Institute for Physical Property research. Pennsylvania State University (1983), http://dippr.byu.edu/

[42] Chen C.C., Britt H.I., Boston J. F., Evans L.B., Local composition model for excess Gibbs energy of electrolyte systems. Part I: Single solvent, single completely dissociated electrolyte systems, AIChE Journal, 1982;28:588-596.

[43] Chen C.C., Evans L.B., A local composition model for the excess Gibbs energy of aqueous electrolyte systems, AIChE Journal, 1986,32:444-454.

[44] Pitzer K., Electrolytes. From dilute solutions to fused salts, J. Am. Chem. Soc., 1980;102:2902-2906.

[45] Chen C.C., Mathias P.M., Orbey H., Use of hydration and dissociation chemistries with the electrolyte-NRTL model, AIChE Journal, 1999;45(7):1576-1586.

[46] Abrams D.S., Prausnitz J.M., Statistical thermodynamics of liquid mixtures: A new expression for the excess Gibbs energy of partly or completely miscible systems, AIChE Journal, 1975;21(3):116-128.

[47] Anderson T.F., Prausnitz J.M., Application of the UNIQUAC Equation to Calculation of Multicomponent Phase Equilibria. 1. Vapor-Liquid Equilibria, I.E.C. Process Des. Dev., 1978;17(4):552-560.

[48] Boston J.F., Mathias P.M., Phase Equilibria in a Third-Generation Process Simulator (1980) Proceedings of the 2nd International Conference on Phase Equilibria and Fluid Properties in the Chemical Process Industries, West Berlin, pp. 823-849.

[49] Bondi A., van der Waals Volumes and Radii, J. Phys. Chem. 1964;68:441-451.

[50] http://www.prosim.net/

[51] Doizi D., Dauvois V., Roujou J.L., Delanne V., Fauvet P., Larousse B., Hercher O., Carles P., Moulin C., Hartmann J.M., Total and Partial Pressure measurements for the sulphur-iodine thermo-chemical cycle. Int. J. Hydrogen Energy. 2007;32(9):1183-1191.

List of table captions

Table 1 : intrinsic properties of pure compounds.

Table 2. Experimental available data in literature for HI_x system and its binary sub-systems.

Table 3. Saturated vapor pressure prediction error using SRK and PR equation of state versus DIPPR correlation.

Table 4. UNIQUAC parameters for the combinatorial term.

Table 5. Calculated and experimental H_2O – HI azeotrope at different temperatures.

Table 1 : intrinsic properties of pure compounds.

	M_W (g.mol^{-1})	P_c (bar)	T_c (°C)	T_b (°C)	T_m (°C)	ω
HI	127.912	82.10	150.70	- 35.60	- 50.77	0.038
I_2	253.809	116.54	546.00	184.41	113.60	0.111
H_2	2.016	13.13	- 239.96	- 252.76	- 259.20	-0.216
H_2O	18.015	220.55	373.98	100.00	0.00	0.345

Table 2. Experimental available data in literature for HI_x system and its binary sub-systems

	Data type	T_{min}-T_{max} (°C)	P_{min}-P_{max} (bar)	Data number	Data source	Used Estim.	Used Valid.
H_2O-HI	vapor – liquid equilibrium (T, P, **x**)	77.8-280.9	0.22-53.80	80	[18]	☑	-
	vapor – liquid equilibrium (T, **x**, **y**)	60.0-126.5	1.013	38	[24]	-	☑
	vapor – liquid equilibrium (T, **x**, **y**)	0.6-126.8	1.013	30	[23]	-	☑
	vapor – liquid equilibrium (P, **x**)	25.0	0.03-7.47	21	[6]	-	☑
	Azeotropic pt	127.0	1.013	1	[20]	-	☑
	LLE (T, **x**, **x'**)	24.0-70.0	-	2	[8]	☑	-
	LLE	25.0	7.47	1	[6]	☑	-
	H^E (**x**)	25.0	-	13	[19]	-	-
H_2O-I_2	LLE (T, **x**, **x'**)	77.1-220.0	-	10	[4]	☑	-
	SLE (T, **x**)	0.0-60.0	-	10	[4]	-	☑
HI-I_2	SLE (T, **x**)	25.0-90.0	-	5	[7]	☑	-
H_2O-HI-I_2	vapor – liquid equilibrium (T, P, **x**)	100-280	0.4-64.0	280	[16]	☑	-
	LLE tie line	24.0-152.1	7.0-62.2	19	[8]	no	no

VLE: Vapor-Liquid equilibrium / LLE: Liquid-Liquid Equilibrium / SLE: Solid-Liquid Equilibrium

Estim. for parameter estimation / Valid. For validation

Table 3. Saturated vapor pressure prediction error using SRK and PR equation of state versus DIPPR correlation

	H_20	HI	I_2
T_{min} (K)	273.16	222.38	386.75
T_{max} (K)	647.13	423.85	819.15
SRK	7.21%	0.58%	2.57%
PR	4.27%	1.82%	1.57%

Table 4. UNIQUAC parameters for the combinatorial term

	r	q (q')
H_2O	0.9200	1.400
HI	1.6724	1.593
I_2	2.5972	1.892

Table 5. Calculated and experimental H_2O – HI azeotrope at different temperatures.

Experimental [5]			**UQsolv model**		
HI molar fraction	T_{azeo} (°C)	P_{azeo} (bar)	HI molar fraction	T_{azeo} (°C)	P_{azeo} (bar)
15.73*	127*	1.013	15.68	128.24	1.013
16.51	100	-	16.20	100.00	0.360
17.68	15-19	-	17.79	15.00	0.004

* Reference [20]

List of figure captions

Figure 1. Sulfur – Iodine thermo-chemical cycle scheme [1].

Figure 2. Solidification curve in mass fraction of H_2O – HI mixtures from Pickering [26] reported in Pascal's monograph [5].

Figure 3. H_2O – I_2 liquid-liquid and solid-liquid equilibrium curves. Comparison between the UQSolv (solid line) and Neumann (dashed line) models and experimental data from Kracek [4] (diamond for solid – liquid equilibrium, triangle for liquid – liquid equilibrium).

Figure 4: Solubility of iodine in hydrogen iodide. Comparison between the ideal liquid (dotted line), standard UNIQUAC (dashed line), UQSolv models (solid line) and experimental data from O'Keefe and Norman [8] (symbol).

Figure 5: Solvation constant versus temperature. Comparison between UQSolv (solid line), Engels' [9] (dotted line) and Neumann's models [17] (dashed line).

Figure 6: H_2O – HI isothermal bubble vapor – liquid equilibrium curves at different temperatures Comparison between PR/MHV2/UQSolv model (solid lines) and experimental data from Wüster [19] (symbol).

Figure 7: Predicted H_2O – HI isobaric liquid – liquid – vapor equilibrium curve at atmospheric pressure. Comparison between UQSolv calculations (solid line), PR/MHV2/UQSolv (dotted line) and experimental points from Carrière and Ducasse [25] (symbols).

Figure 8: Predicted H_2O – HI isotherm liquid – vapor equilibrium curve at 25°C. Comparison between UQSolv model (solid line) and experimental data from Haase [6] (symbol).

Figure 9: PR/MHV2/UQSolv model relative deviation for the total pressure for the experimental H_2O – HI – I_2 ternary data of Engels and Knoche [18] available in the Neumann's manuscript [17]. The line is merely a trend of the model's calculations.

Figure 10: Predicted H_2O – HI – I_2 liquid – liquid equilibrium data at 43bar. Comparison between PR/MHV2/UQSolv model (square symbol and dashed line) and experimental data circa 121°C from [8] (diamond symbol and solid line).

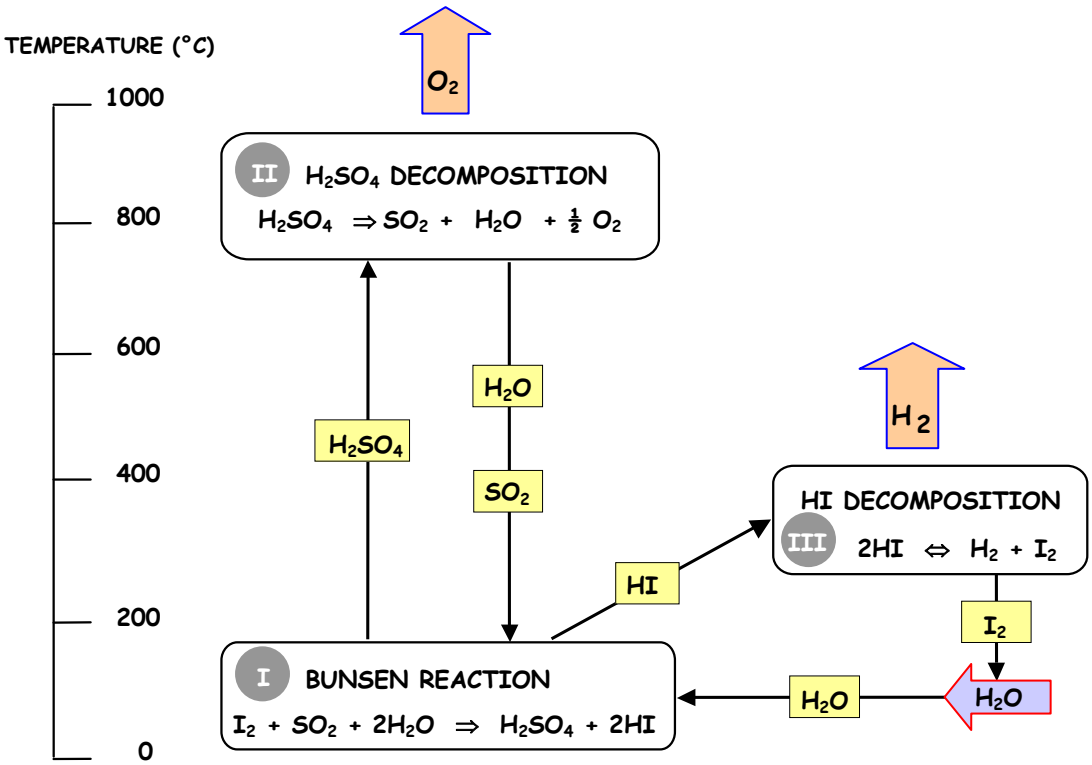

Figure 1. Iodine - Sulfur thermo-chemical cycle scheme [1].

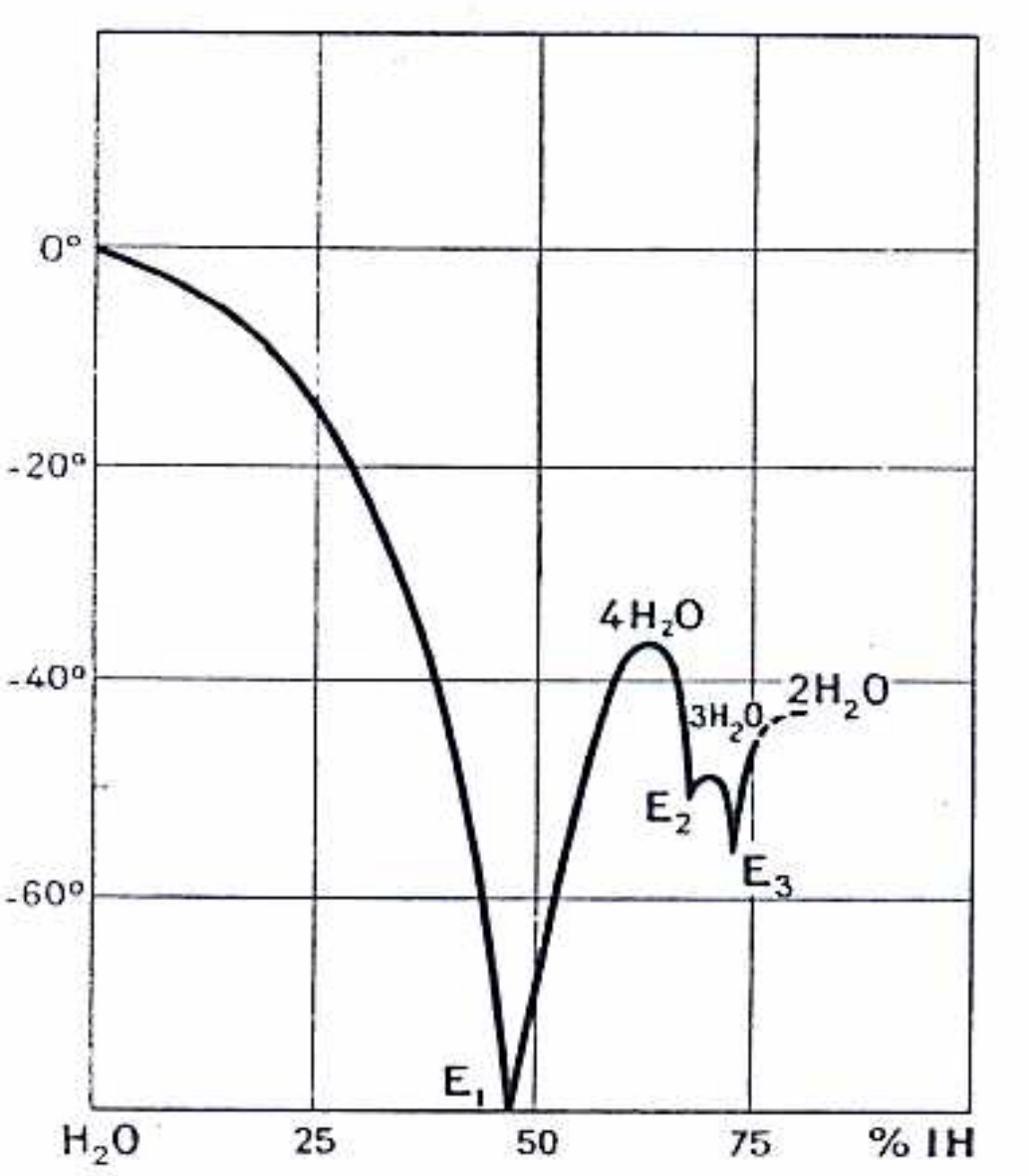

Figure 2. Solidification curve in mass fraction of H_2O – HI mixtures from Pickering [25] reported in Pascal's monograph [5].

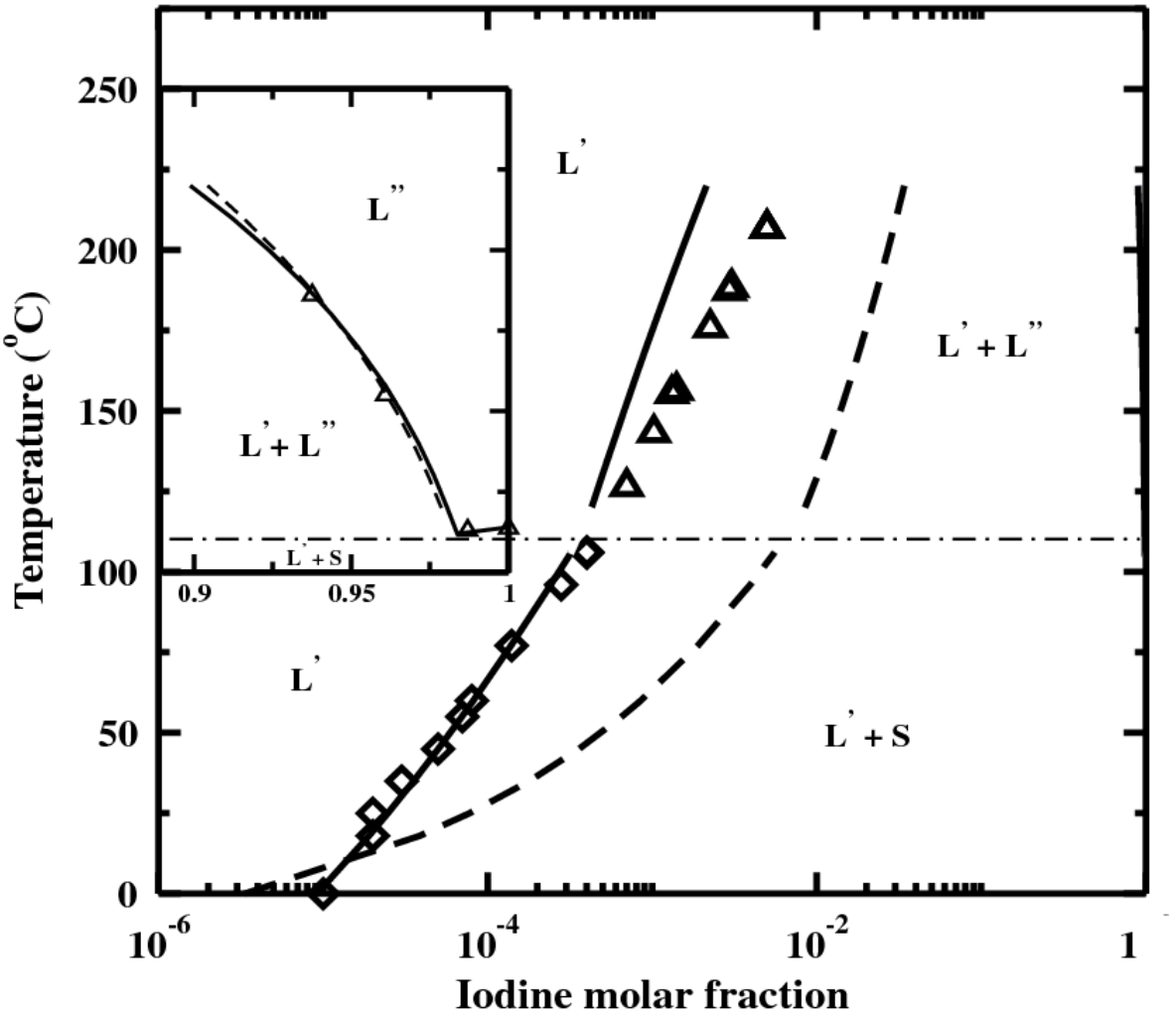

Figure 3. H_2O – I_2 liquid-liquid and solid-liquid equilibrium curves. Comparison between the UQSolv (solid line) and Neumann (dashed line) models and experimental data from Kracek [4] (diamond for solid – liquid equilibrium, triangle for liquid – liquid equilibrium).

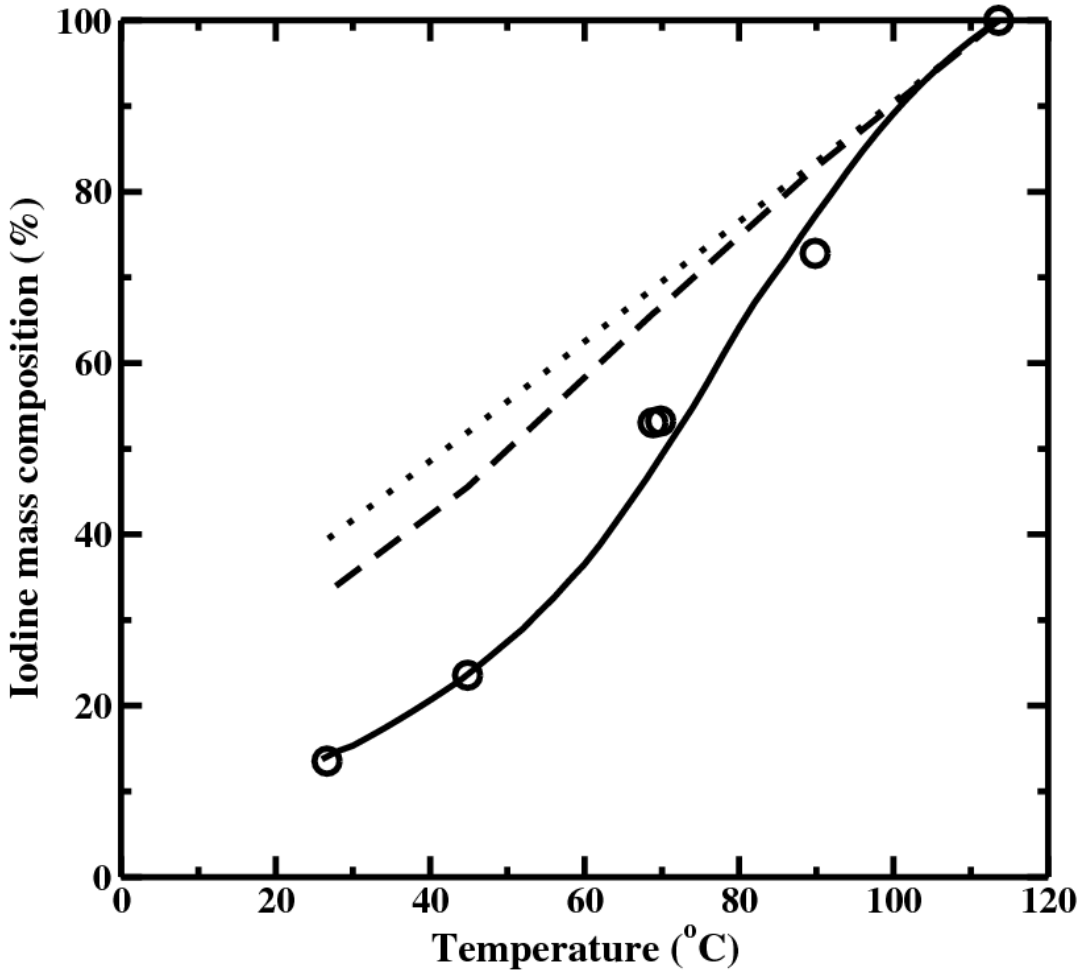

Figure 4: Solubility of iodine in hydrogen iodide. Comparison between the ideal liquid (dotted line), standard UNIQUAC (dashed line), UQSolv models (solid line) and experimental data from O'Keefe and Norman [8] (symbol).

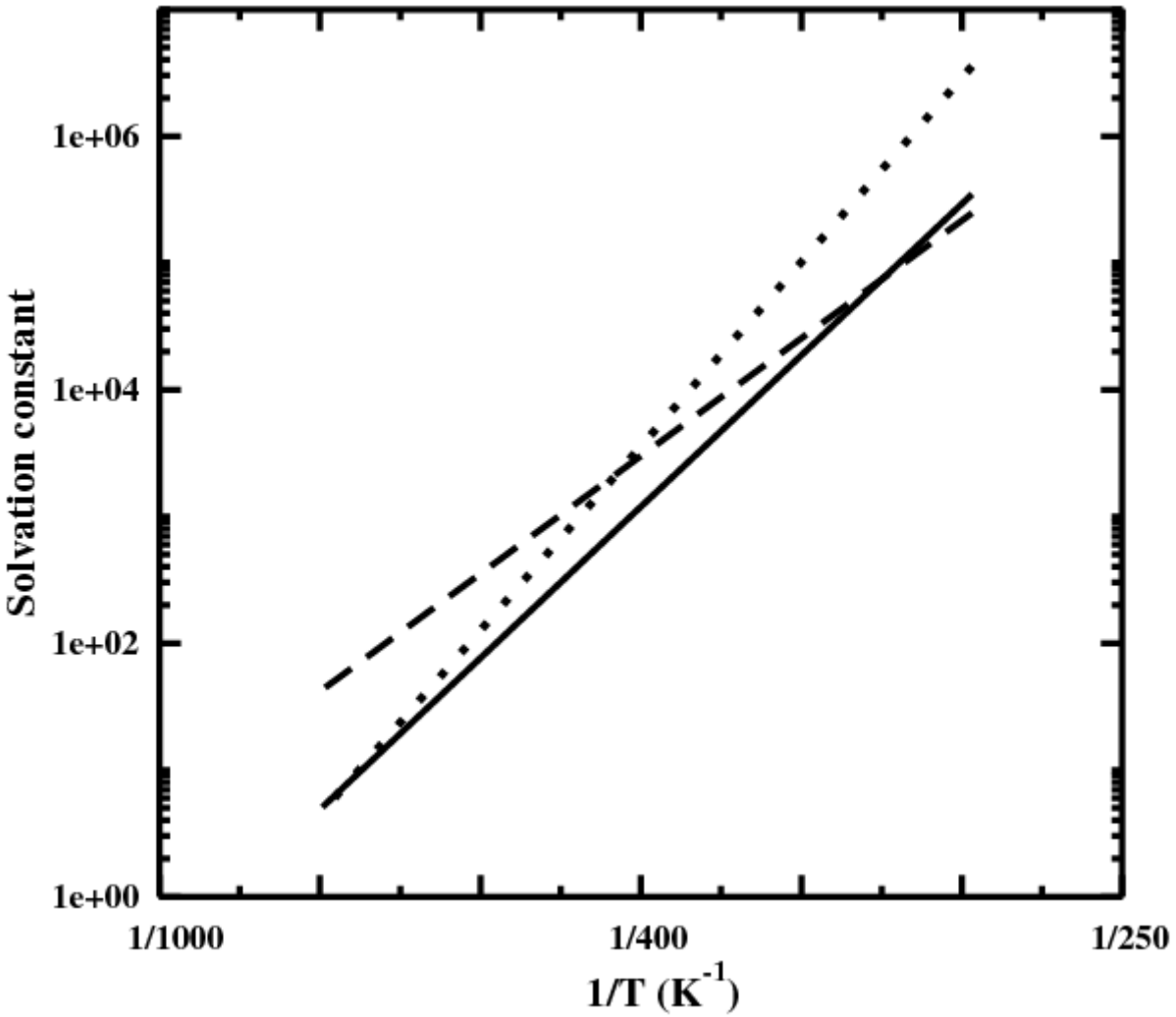

Figure 5: Solvation constant versus temperature. Comparison between UQSolv (solid line), Engels' [9] (dotted line) and Neumann's models [16] (dashed line).

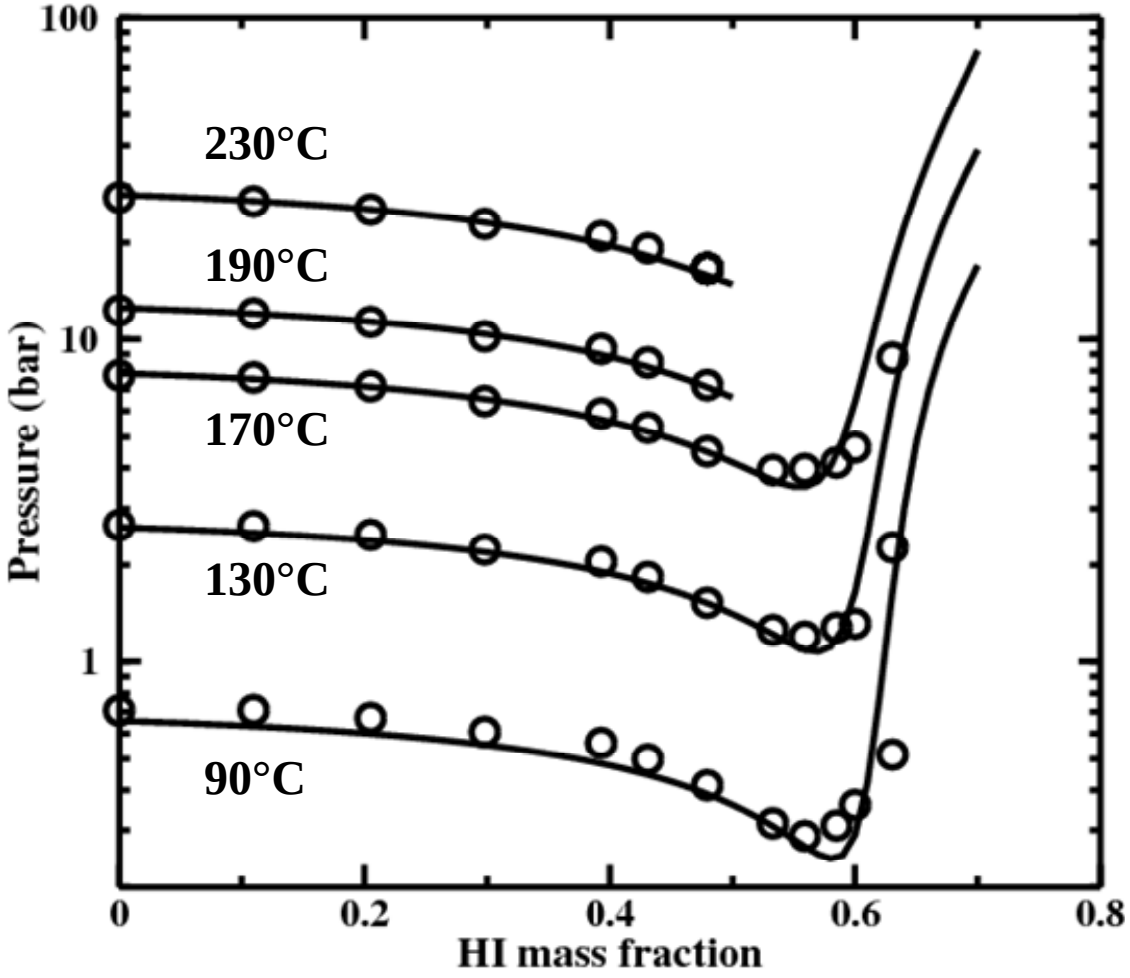

Figure 6: H_2O – HI isothermal bubble vapor – liquid equilibrium curves at diyfferent temperatures Comparison between PR/MHV2/UQSolv model (solid lines) and experimental data from Wüster [18] (symbol).

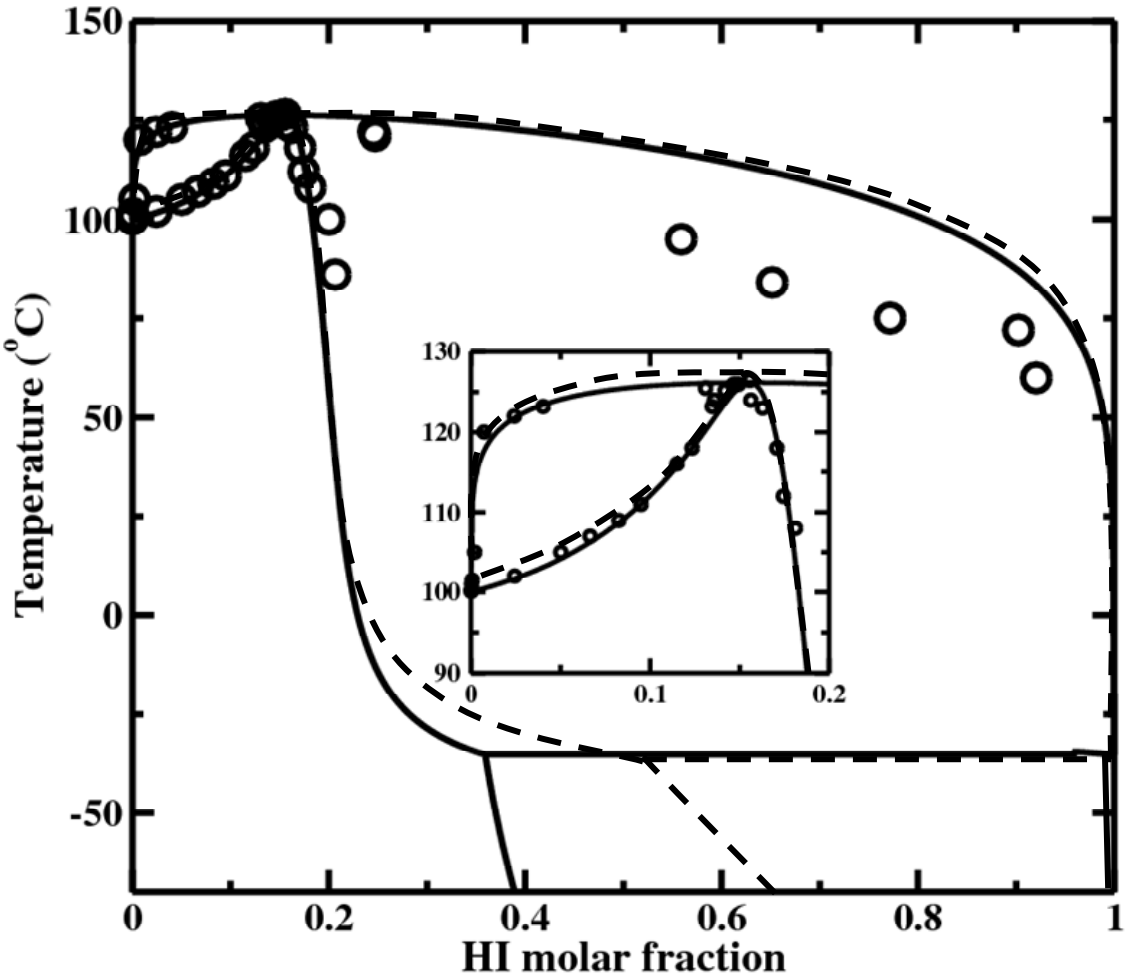

Figure 7: Predicted H_2O – HI isobaric liquid – liquid – vapor equilibrium curve at atmospheric pressure. Comparison between UQSolv calculations (solid line), PR/MHV2/UQSolv (dotted line) and experimental points from Carrière and Ducasse [24] (symbols).

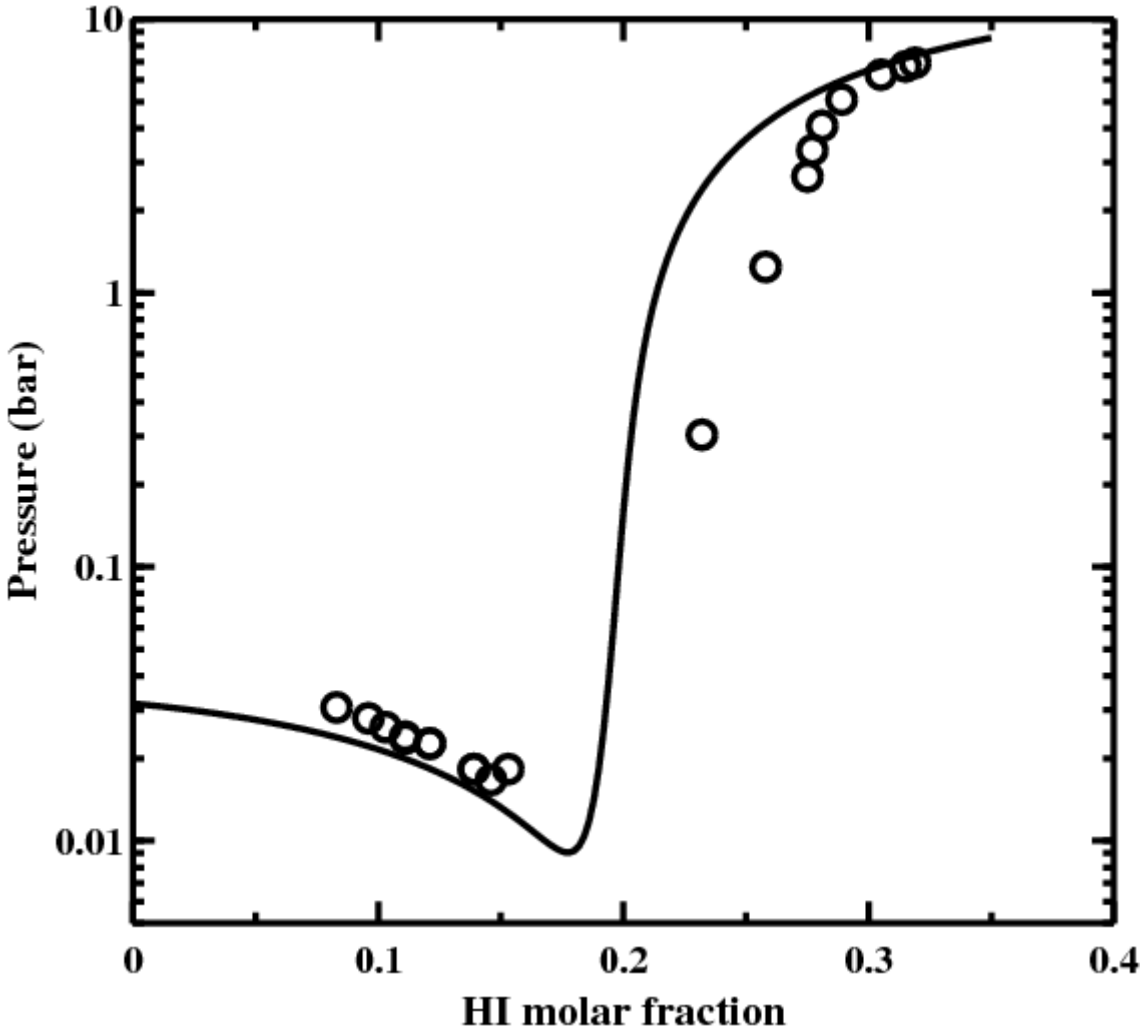

Figure 8: Predicted H_2O – HI isotherm liquid – vapor equilibrium curve at 25°C. Comparison between UQSolv model (solid line) and experimental data from Haase [6] (symbol).

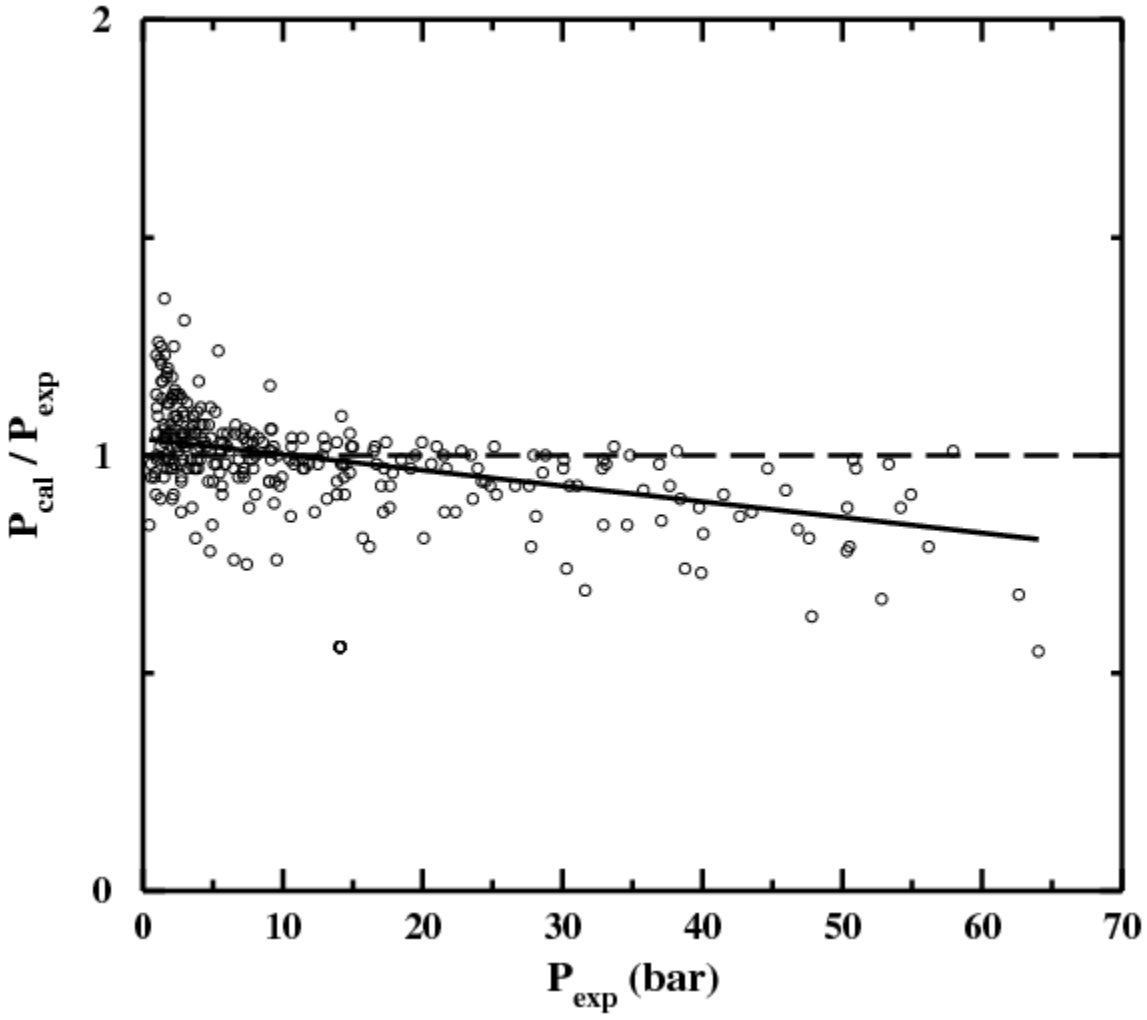

Figure 9: PR/MHV2/UQSolv model relative deviation for the total pressure for the experimental H_2O – HI – I_2 ternary data of Engels [17] available in the Neumann's manuscript [16]. The line is merely a trend of the model's calculations.

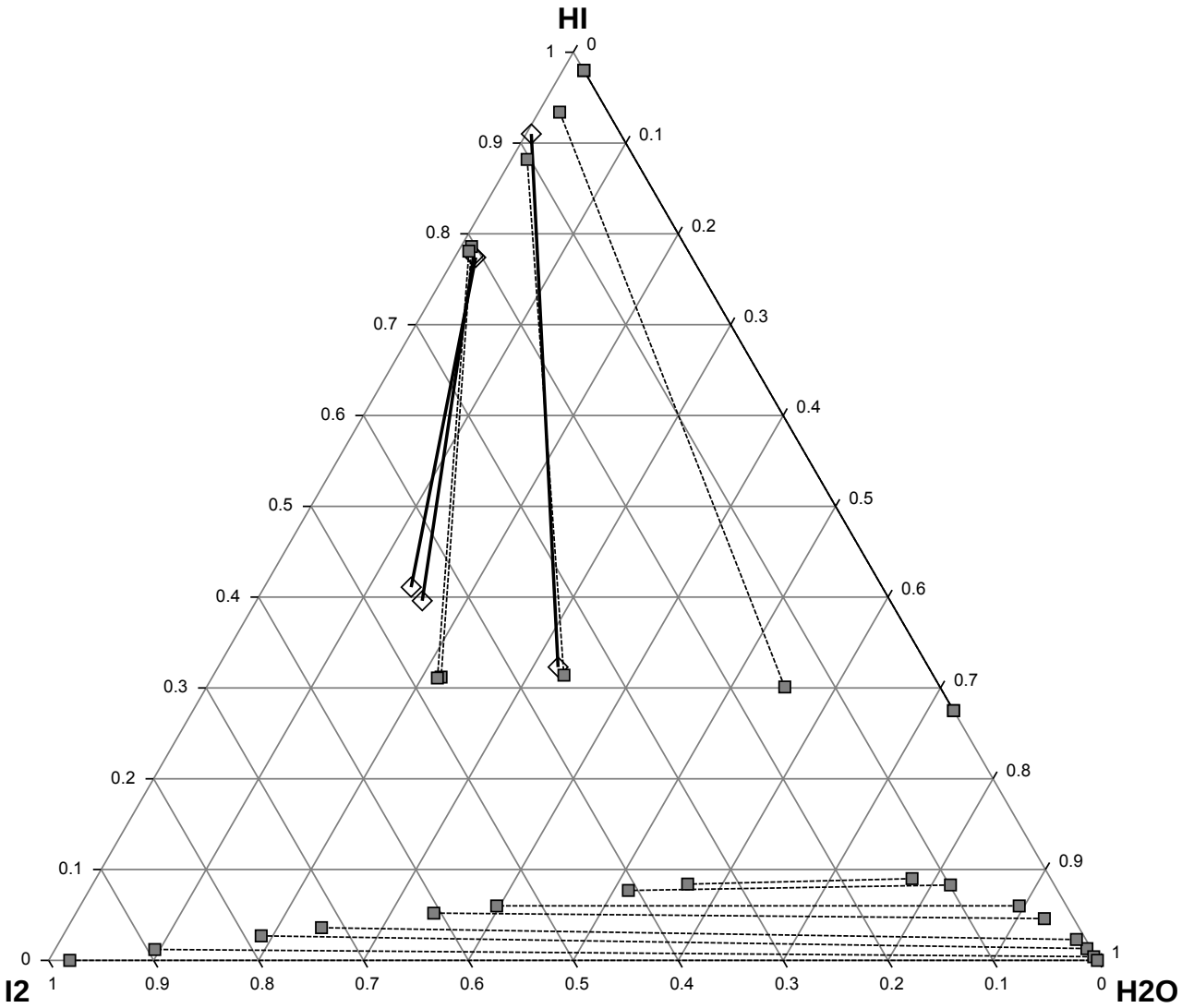

Figure 10: Predicted H_2O – HI – I_2 liquid – liquid equilibrium data at 43bar. Comparison between PR/MHV2/UQSolv model (square symbol and dashed line) and experimental data from [8] (diamond symbol and solid line).